

Lawrence Berkeley National Laboratory

Recent Work

Title

LDA STUDY OF NON-STEADY FLAME PROPAGATION IN A CONSTANT VOLUME DUCT

Permalink

<https://escholarship.org/uc/item/0sg6x08h>

Authors

Dunn-Rankin, D.

Cheng, R.K.

Sawyer, R.F.

Publication Date

1984-09-01

UC-926
LBL-18150
c.1



Lawrence Berkeley Laboratory

UNIVERSITY OF CALIFORNIA

APPLIED SCIENCE DIVISION

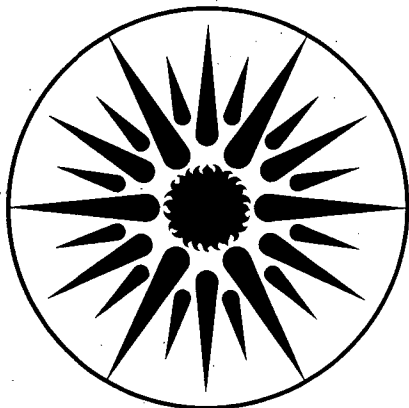
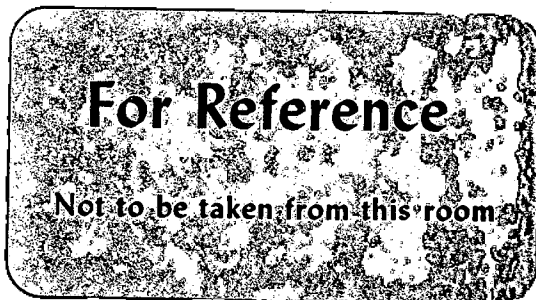
RECEIVED
LAWRENCE
BERKELEY LABORATORY
FEB 11 1985
LIBRARY AND
DOCUMENTS SECTION

Presented at the 2nd International Symposium on
Applications of Laser Doppler Anemometry to
Fluid Mechanics, Lisbon, Portugal, July 2-4, 1984

LDA STUDY OF NON-STEADY FLAME PROPAGATION IN
A CONSTANT VOLUME DUCT

D. Dunn-Rankin, R.K. Cheng, and R.F. Sawyer

September 1984



APPLIED SCIENCE
DIVISION

LBL-18150
c.1

DISCLAIMER

This document was prepared as an account of work sponsored by the United States Government. While this document is believed to contain correct information, neither the United States Government nor any agency thereof, nor the Regents of the University of California, nor any of their employees, makes any warranty, express or implied, or assumes any legal responsibility for the accuracy, completeness, or usefulness of any information, apparatus, product, or process disclosed, or represents that its use would not infringe privately owned rights. Reference herein to any specific commercial product, process, or service by its trade name, trademark, manufacturer, or otherwise, does not necessarily constitute or imply its endorsement, recommendation, or favoring by the United States Government or any agency thereof, or the Regents of the University of California. The views and opinions of authors expressed herein do not necessarily state or reflect those of the United States Government or any agency thereof or the Regents of the University of California.

LDA STUDY OF NON-STEADY FLAME PROPAGATION IN A CONSTANT VOLUME DUCT

D. Dunn-Rankin*, R.K. Cheng, and R.F Sawyer*

Lawrence Berkeley Laboratory, Applied Science Division

* also University of California, Department of Mechanical Engineering
Berkeley, CA 94720

This work was supported by the Assistant Secretary for Conservation and Renewable Energy, Office of Transportation Programs, Division of Transportation Energy of the U.S. Department of Energy under contract number DE-AC03-76SF00098. One of the authors (RKC) was supported by the Director, Office of Energy Research, Office of Basic Energy Sciences, Chemical Sciences Division of the U.S. Department of Energy under contract number DE-AC03-76SF00098.

ABSTRACT

This work investigates the development of "tulip" shaped flames during laminar flame propagation in a closed duct. In particular the interaction of a laminar flame front with its self-induced non-steady flow field is examined as a possible source of the "tulip" phenomenon. The flame generated flow is measured with a laser Doppler anemometer (LDA). The flame shape and its position are recorded with high-speed schlieren cinematography. Comparison of the qualitative schlieren and the quantitative LDA data records provides insight into the flame/flow relationship.

INTRODUCTION

The formation of "tulip" shaped flames is a well known phenomenon associated with non-steady flame propagation in closed tubes and ducts. The qualitative features of such flames have been documented by various investigators for nearly sixty years (Ellis, 1928; Guenoche 1964). Despite the long history of qualitative investigations concerned with "tulip" shaped flames, explanations for this interesting phenomenon remain unsatisfactory. Speculations about the causes of "tulip" flames include: spontaneous instability of the flame front; flame generated pressure waves impinging on the flame after being reflected from the closed end of the vessel; and the interaction of combustion driven fluid circulation with the flame. Part of the difficulty in analyzing the "tulip" flame has been the lack of quantitative information about the flow field in which it forms. The objective of this work is to quantify the non-steady flow field generated by laminar flame propagation in a closed duct using laser Doppler anemometry. The formation of the "tulip" flame is recorded separately with high-speed schlieren cinematography. Correlation of the flame shape with the velocity data helps to determine the relationship between the flow field and the "tulip" flame.

The change in flame shape referred to as "tulip" formation is shown in Figure 1. The photograph is a composite of several frames extracted from one of the high-speed schlieren movies of Steinert et. al. (1982). Below the photograph is the digitized flame shape history from the same high-speed movie. The stoichiometric methane/air flame is initiated by a distributed spark line igniter at one end of a square cross-section closed duct. Initially, the flame kernel is semi-cylindrical and expands symmetrically. As the flame front approaches the side walls it rapidly elongates in the axial direction. Part of the flame then quenches at the side walls of the duct, and the flame flattens into a planar front. The transition to a planar flame is accompanied by a rapid reduction in flame area and a decrease in the axial flame advancement rate. A sharp cusp then forms at the center of the flame with its point toward the burned gas. The cusp gradually becomes more pronounced and produces a "tulip" shaped flame. The flame retains its "tulip" form for the remainder of the propagation.

Various studies have shown that "tulip" flame formation is relatively independent of igniter geometry: a "tulip" forms in tube combustion initiated by both a point igniter (Ellis, 1928) and a distributed point line igniter (Smith, 1977, Woodard et. al., 1981, Steinert et. al., 1982). In this work "tulip" flame formation initiated by a two-point igniter is studied.

APPARATUS

The experimental apparatus, Figure 2, consists of a laser Doppler anemometer (LDA), a high-speed schlieren cinematographic system, a combustion chamber, a spark ignition source, a gas mixing device, and a data logging computer.

The schlieren system is composed of two spherical mirrors, a point light source, a vertical knife edge stop and a high-speed (5000 frames/s) movie camera. The system is arranged in a standard Z-configuration. Details of the schlieren system are described in Smith (1977). The combustion chamber is 38 mm square by 150 mm and is constructed of 12.7 mm plexiglas to allow optical access from two orthogonal directions. The chamber is identical in size to the combustion vessel used by Steinert et. al. (1982) to produce the "tulip" flame shown in Figure 1. A two point igniter is situated near one end-wall of the chamber, Figure 2a. Flame initiation occurs simultaneously at the two spark gaps located near opposing side walls of the duct. The high voltage (40 kV) ignition source is a capacitive discharge device with approximately 200 mJ stored energy. A stoichiometric mixture of methane/air is delivered by the gas mixing device which controls the equivalence ratio by flow rotameters.

The LDA set-up is similar to that described by Cheng and Ng (1983). A 4 watt argon-ion laser operated at 514 nm is used. The LDA probe is formed with a beam splitter of 50 mm fixed separation and a 250 mm focal length lens. It is arranged to measure the axial velocity, U . The two beams are frequency shifted by Bragg cells to remove directional ambiguity. The differential frequency is 2 MHz. Doppler scattering sites are provided by 0.3 micron aluminum oxide particles introduced into the inlet methane/air flow by a spouted bed seeder. The collection system includes a lens, filter and photomultiplier tube placed in the forward scattering direction. The Doppler signal is analyzed by a TSI 1980A frequency counter. An analog to digital converter and a PDP 11/10 computer are used to digitize and record the analog output of the counter.

METHODOLOGY

The duct is purged with fresh mixture for a time sufficient for 20 complete changes of contents. The LDA seed is introduced during the latter stages of the purging process. After purging, all valves are closed and the gas motion is allowed to subside. The mixture is ignited when the counter output is consistent with zero velocity and a visual check of the movement of seed particles near the LDA probe volume verifies a nearly quiescent initial state.

The ignition source simultaneously initiates combustion and triggers the data acquisition system. The analog LDA output is digitized at 30 khz from $t = 0$ (the time of ignition) to $t = 250$ ms. Measurements are taken along the central axis of the chamber at 10 mm increments from $X = 20$ mm to $X = 140$ mm, with X measured from the igniter end-wall. The measurement is repeated five times at each location to determine the run to run variations.

The flame is photographed from two perpendicular planes to remove the ambiguity which arises from line-of-sight integration inherent in the schlieren technique (Guenoche, 1954). The photographic planes are the X-Y and X-Z planes shown in Figure 2a. Two movies in each plane are taken to determine the reproducibility of the qualitative features of the "tulip" formation.

DATA ANALYSIS

The digitized counter output must be analyzed to extract the true validated velocity measurement. The extraction is required because the LDA counter validations occur at random intervals while the LDA output signal is sampled at a constant rate. An indication of a new validation and the criterion for extraction is that a recorded value differ from the preceding point by more than the expected uncertainty in the A/D converter. Data points showing exceedingly large deviations associated with noise are not selected. The digitized counter output and the extracted data from a typical experiment are compared in Figure 3. The area of data dropout near $t = 20$ ms occurs as the flow velocity approaches zero. The dropout is caused by the reduced particle arrival rate associated with low velocity flow.

A cubic spline smoothing routine (Reinsch, 1967) is used to fit the extracted data points. Figure 4 shows individual validated measurements (dots) and a smooth spline fit (solid). Also noted in Figure 4 are three characteristic features of the velocity/time records which will be discussed later: the maximum velocity reached after ignition, U_{max} , the time at which this maximum occurs, T_{umax} , and the time of the first velocity zero crossing, T_{cr} .

Each experiment produces a different spline fit. All fits for a single measurement location are averaged to produce a representative curve for that location, Figure 5a. The scatter in the smooth curves reproduces the run to run scatter of the raw data. The run to run scatter is represented by the standard deviation of the individual smooth curves about the representative average curve, Figure 5b. There is very little run to run variation for data taken when $X > 80$ mm. There is larger run to run variation for $X < 80$ mm, Figure 6, but all measurements are extremely reproducible until some time after the first velocity zero crossing, T_{cr} .

Flame shape and position are determined from high-speed movies of the flame propagation. Flame position, X_f , is taken as the flame location at the centerline of the duct. Movies showing the X-Z plane, are consistent with the "tulip" sequence described earlier and reported in the literature. Movies showing the X-Y plane display two-point ignition effects followed by a "tulip" formation. The centerline flame trajectory recorded in all movies is highly reproducible after the ignition effects disappear, Figure 7. Both X-Y and X-Z films show the "tulip" forming at the same time and location. The discrepancy in the two trajectories for $t < 15$ ms is due to the two point ignition. The X-Y movie shows two separate flame kernels growing toward the duct center and coalescing into a single front at $t = 15$ ms. The centerline flame position is not well defined before the two flames join. The centerline flame position is always defined in the X-Z orientation as only a single flame front can be distinguished.

The high degree of reproducibility in the LDA results and high-speed movies allows correlation of flame shape and position with gas velocity.

RESULTS

The flame displays three distinct stages of propagation: (1) an initiation period, where the flame area increases from an ignition kernel to its maximum extent, (2) a transition period, where the flame area decreases rapidly due to both quench at the combustion vessel walls and coalescence of separate flame kernels into a single front, (3) a "tulip" period, where the flame flattens and folds into its characteristic "tulip" shape. The three stages may be delineated by the axial location of the flame, X_f : (1) $X_f < 50$ mm, (2) 50 mm $< X_f < 80$ mm, (3) 80 mm $< X_f < 150$ mm. X_f is taken from the X-Z trajectory shown in Figure 7. All of the average velocity/time results are shown in Figure 8. The results are grouped according to whether the LDA measurement was taken at an X-location in range (1), (2), or (3) above.

All velocity/time curves show a distinct initial peak in gas velocity. The maximum velocity, U_{max} , and the time that the maximum occurs, T_{umax} , behave differently in the three groups described above. In group (1), U_{max} and T_{umax} increase with X. Further U_{max} coincides with the arrival of the flame. In group (2), both U_{max} and T_{umax} are nearly constant. In group (3), T_{umax} is constant and U_{max} decreases with X. The relationship between T_{umax} and T_f for different X-locations is shown in Figure 9. These results are in agreement with the results of a similar study carried out by Starke and Roth (1984).

The initial increase and decrease in gas velocity corresponds to the increase and decrease in flame area during the initiation stage (1) and transition stage (2) of the flame propagation. As unburned gas is consumed by the flame, the hot combustion products expand behind the flame interface. The expansion drives the interface forward, compressing the unburned gas ahead of it. The expansion also compresses the previously burned gas away from the interface in the opposite direction. During the initiation period the flame area is continually increasing. This leads to an increase in the rate of unburned gas consumption which produces an increase in the rate of burned gas expansion. The flame interface is moved forward rapidly by this expansion, as shown in the trajectories of Figure 7. The rapid movement of the flame accelerates the unburned gas ahead of it. During the transition period, the flame area rapidly decreases and the flame's forward motion slows. The slowing of the flame causes a decrease in the gas velocity ahead of it. In group (1) the velocity increase appears to be terminated by the flame arrival, Figure 8a. This is because the flame area is continually increasing while group (1) X-locations are in the unburned gas. Consequently the gas at those points continually accelerates. Once the flame passes the measurement point however, the gas there begins to be compressed away from the flame front in the negative direction and no further positive acceleration is possible.

The relationship between the time of flame arrival, T_f , and the time of velocity zero crossing, T_{cr} , is shown in Figure 9. The time of flame arrival is taken from the centerline flame trajectory in the X-Z plane. For $X < 90$ mm the flow does not become negative until approximately 5-8 ms after the flame arrives, but for $X > 90$ mm the flow becomes negative before the flame arrives. The transition point ($X = 90$ mm) corresponds to the early stages of the flame transformation to a "tulip" shape.

Centerline Velocity Profiles

Based on the reproducibility of the LDA measurements, the velocity/time measurements from different experiments are combined to give a time history of the centerline axial velocity profile. These profiles and the corresponding frames from one of the X-Y schlieren movies are shown in Figure 10. The length of the error bars in the velocity profiles indicate the standard deviation of the measurement as previously described. Fluid to the left of the centerline flame position shown by the schlieren is considered burned gas and fluid to the right of the flame is unburned gas. The flame location at the centerline is imprecise due to the finite thickness schlieren image and is taken as the dark region at the centerline nearest the unburned gas.

For the first 15 ms the unburned gas velocity decreases nearly linearly from a maximum at the flame to zero at the end-wall. At 20 ms the unburned gas velocity drops to a small constant value (approximately 1 m/s) and the velocity just ahead of the flame becomes negative. Two cusps form in the flame at 20 ms. The cusps become more pronounced and grow together to form the "tulip" flame through 40 ms. From 20 ms to 40 ms the unburned gas which is beyond the "tulip" maintains a small, approximately constant positive velocity, indicating that the transition to a full "tulip" flame does not noticeably influence the unburned velocity field ahead of the "tulip" cusp. The "tulip" shape is maintained for the remainder of the flame propagation. A flow reversal occurs in the burned gas beginning at approximately 45 ms. The reversal becomes more and more dominant from 45 ms to 60 ms. Small vortices in the burned gas are noticeable around $X = 50$ mm for $t > 40$ ms. The vortices are accompanied by a small dip in the velocity results and an increase in the uncertainty of the measurements. The appearance of vortices is consistent with the predicted production of vorticity by a curved flame front (Tsien, 1951).

DISCUSSION

During the early stages of the combustion ($t < 20$ ms) the flame seems to drive the flow. The rapid increase and subsequent decrease in flame area during the initiation and transition stages of flame propagation cause an increase and decrease in the gas velocity at all of the measurement points along the duct centerline. During the flame transition to a "tulip" shape, however, the flame does not seem to influence the flow field. The "tulip" shape forms over a period of approximately 15 ms ($t : 20$ ms to $t : 35$ ms) with no noticeable change in the unburned gas centerline axial velocity profile. This suggests that the "tulip" transition is the adaptation of the flame to a flow field that is already present. For $t > 20$ ms the flow velocity within the "tulip" flame cusp is negative, while the flow farther ahead of the flame remains positive, Figure 10. This result suggests a small fluid circulation localized just ahead of the flame. Further measurements of fluid velocity off-centerline as well as components perpendicular to the axial direction are necessary to characterize this possible circulation. In addition, a precise identification of the flame proximity to the measurement location is required to assess accurately the relationship of the flame to the flow field just ahead of it. These refinements will be carried out in a future study.

CONCLUSIONS

Laser Doppler anemometry has been used to measure the axial component of flame induced non-steady flow during constant volume laminar flame propagation in a closed duct. These velocity measurements are compared with the flame shape and position obtained from high-speed schlieren movies. The comparison helps clarify the influence of the gas flow on "tulip" flame formation.

The first indication of "tulip" flame formation occurs approximately 20 ms after ignition. The complete "tulip" shape is formed at $t = 35$ ms. During the "tulip" transition the centerline flame position, X_f , moves from $X = 80$ mm to $X = 100$ mm. The flow field shows distinct differences for values on either side of the transition point $X_f = 80$ mm and $t = 20$ ms.

Before the start of the "tulip" formation ($t < 20$ ms) the features of the gas flow field are:

- 1) There is a characteristic flame driven surge of flow velocity during the early stages of the flame propagation which corresponds to the increase and decrease in flame area following ignition. Near the igniter ($X < 80$ mm) the time of maximum velocity, T_{umax} , occurs almost simultaneously with the flame arrival, T_f . Far from the igniter ($X > 80$ mm) T_{umax} is nearly constant and is not associated with the flame arrival.
- 2) The flow is positive before the flame arrives and negative after it passes, where positive is in the direction of flame travel.
- 3) The unburned gas velocity decreases linearly from a maximum at the flame front to zero at the end-wall.

Following the first indication of a "tulip" formation ($t > 20$ ms), the notable features of the unburned gas flow field become:

- 1) The velocity is small and nearly constant for all locations ahead of the flame cusp.
- 2) The velocity is negative ahead of the flame in the localized region bounded by the curved lobes of the flame cusp and positive farther ahead of the flame.
- 3) The "tulip" transformation continues from $t = 20$ ms to $t = 35$ ms with no obvious effect on the flow field ahead of the flame.
- 4) Vortices are noticeable in the burned gas after 40 ms.

The results indicate that the flame drives the flow field until a transition point is reached at $t = 20$ ms or $X_f = 80$ mm. After this point the flame has very little influence on the centerline velocity profile in the

unburned gas and rather seems to adapt itself to the velocity field present. A local circulation within the "tulip" cusp may be responsible for sustaining the "tulip" shaped flame. Further insight into the precise mechanism of the flow field generation and the causes of the transition point requires off-centerline velocity measurements as well as velocity measurements tangential to the flame front.

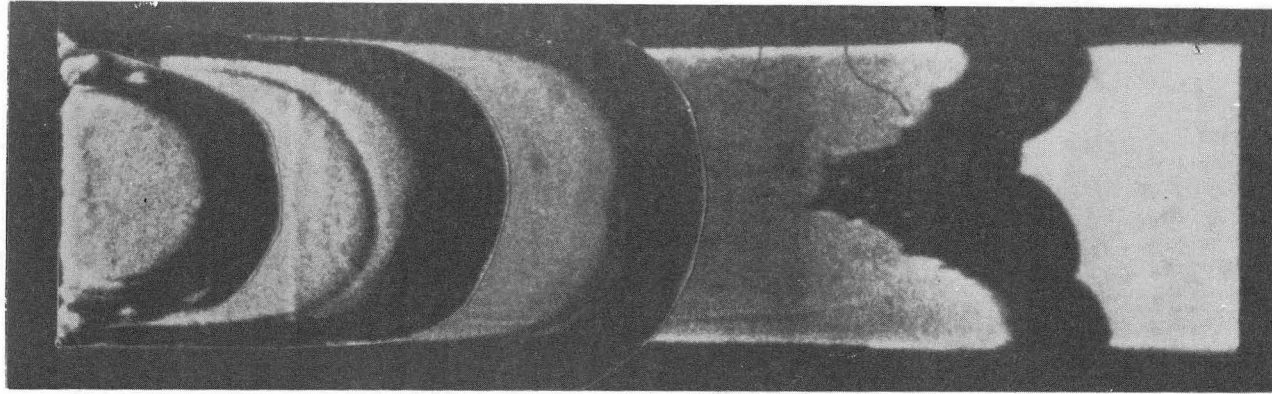
ACKNOWLEDGEMENTS

This work was supported by the Assistant Secretary for Conservation and Renewable Energy, Office of Transportation Programs, Division of Transportation Energy of the U.S. Department of Energy under contract number DE-AC03-76SF00098. One of the authors (RKC) was supported by the Director, Office of Energy Research, Office of Basic Energy Sciences, Chemical Sciences Division of the U.S. Department of Energy under contract number DE-AC03-76SF00098.

REFERENCES

- Cheng, R.K., Ng, T.T.** (1983). "Velocity Statistics in Premixed Turbulent Flames." Combustion and Flame, 52, 2, 185-202.
- Ellis, O.C. de C.** (1928). "Flame Movement in Gaseous Explosive Mixtures (Part 7)." Fuel; a journal of fuel science, 7, 6, 502-508.
- Guenoche, H.** (1964). "Flame Propagation in Tubes and Closed Vessels." Non-Steady Flame Propagation, G.H. Markstein editor, Pergamon Press, New York.
- Guenoche, H., Jouy, M.** (1954). "L'Utilisation de la Methode du Tube pour la Mesure des Vitesses de Deflagration." Rev. Inst. Franc. Petrole, IX, 10, Octobre.
- Smith, O.I.** (1977). "Lean Limit Combustion in an Expanding Chamber." Lawrence Berkeley Laboratory Report No. LBL-6851, PhD Thesis, College of Engineering, University of California, Berkeley.
- Starke, R., Roth, P.** (1984). "LDA - Measurements in Cylindrical Vessel Explosions." Second International Symposium on Applications of Laser Doppler Anemometry to Fluid Mechanics. July 2-4, Lisbon, Portugal.
- Steinert, W., Dunn-Rankin, D., Sawyer, R.F.** (1982). "Influence of Chamber Length and Equivalence Ratio on Flame Propagation in a Constant Volume Duct." Western States Section/The Combustion Institute Paper No. 82-52 and Lawrence Berkeley Laboratory Report No. LBL-14965.
- Tsien, H.** (1951). "Influence of Flame Front on the Flow Field". Journal of Applied Mechanics, 18, 188-194.
- Woodard, J.B., Hirvo, D.H., Greif, R., Sawyer, R.F.** (1981). "Wall Heat Transfer and Flame Propagation in a Constant Volume Duct." Western States Section/The Combustion Institute Paper No. 81-51 and Lawrence Berkeley Laboratory Report No. LBL-13201.

(a)



(b)

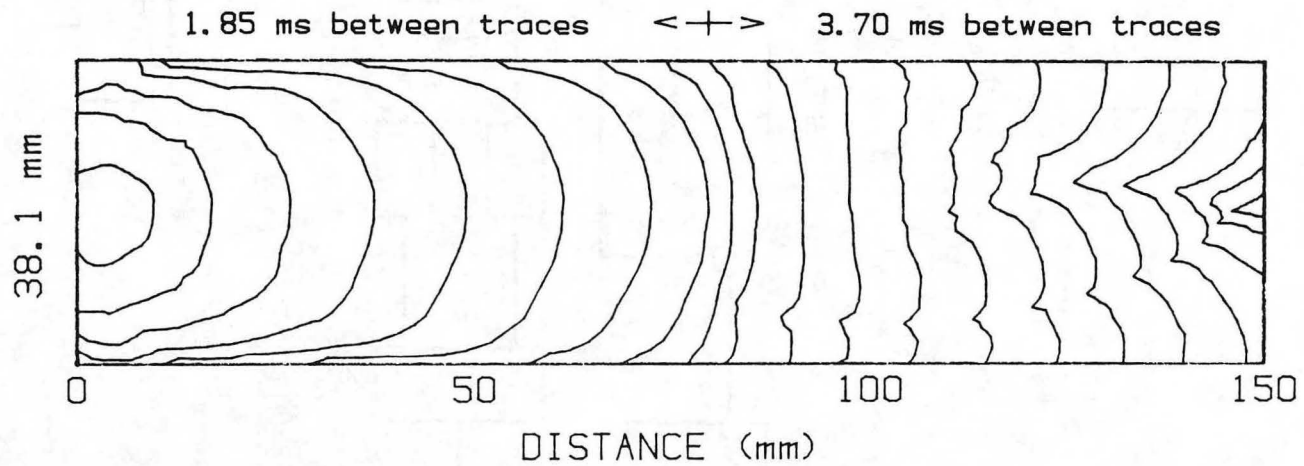
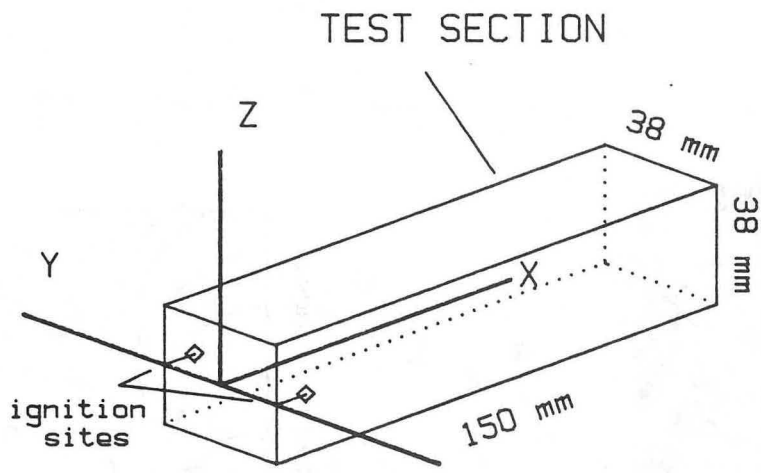
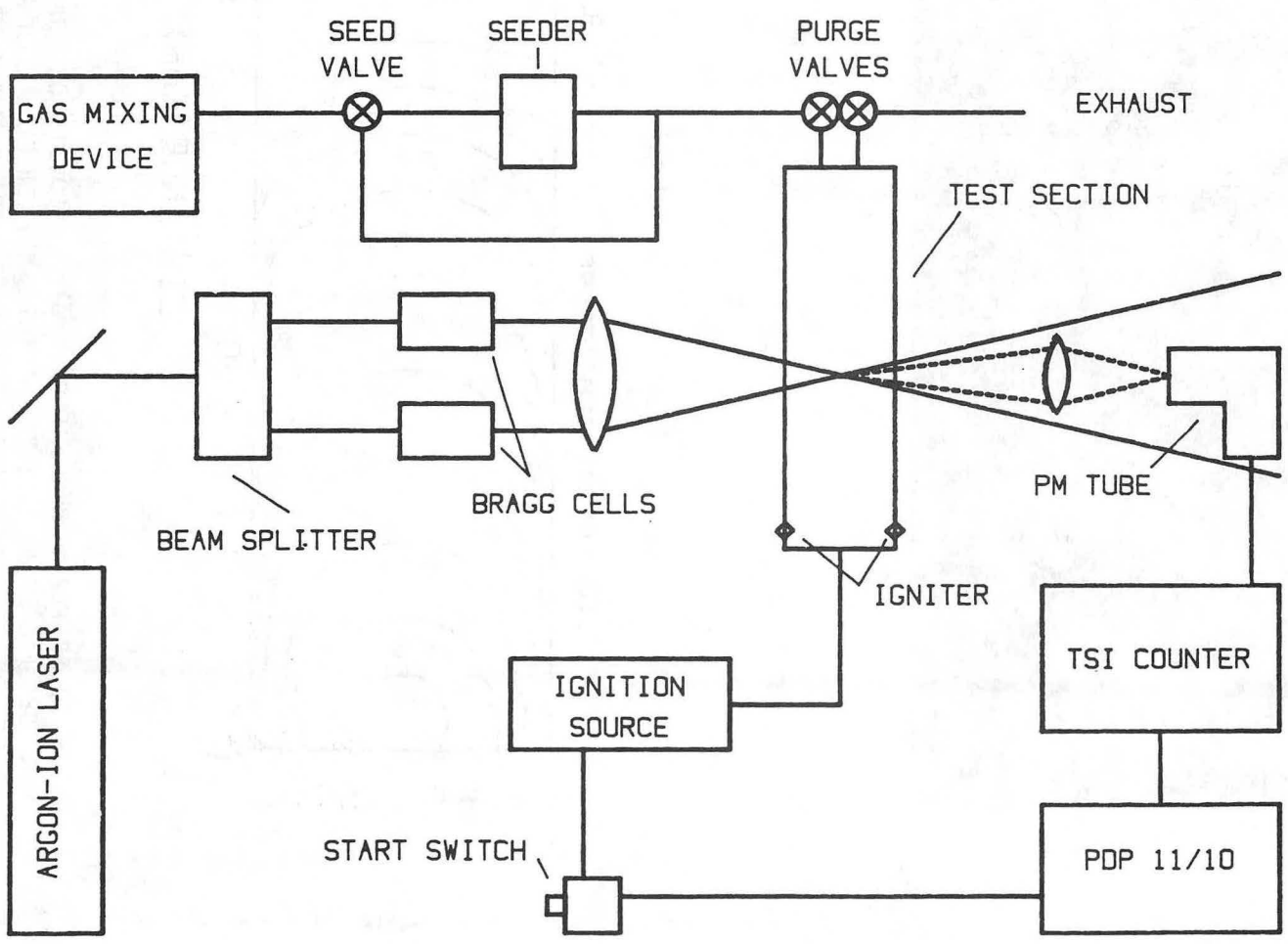


FIGURE 1. THE TULIP FLAME PHENOMENON. a) COMPOSITE OF FRAMES TAKEN FROM HIGH-SPEED SCHLIEREN MOVIE OF A STOICHIOMETRIC METHANE/AIR FLAME IN A CLOSED DUCT. b) DIGITIZED FLAME LOCATION FROM THE SAME HIGH-SPEED MOVIE. FROM STEINERT et. al. (1982).



(a)



(b)

FIGURE 2. a) CO-ORDINATE LAYOUT OF COMBUSTION VESSEL.
 b) SCHEMATIC OF LASER DOPPLER ANEMOMETER.

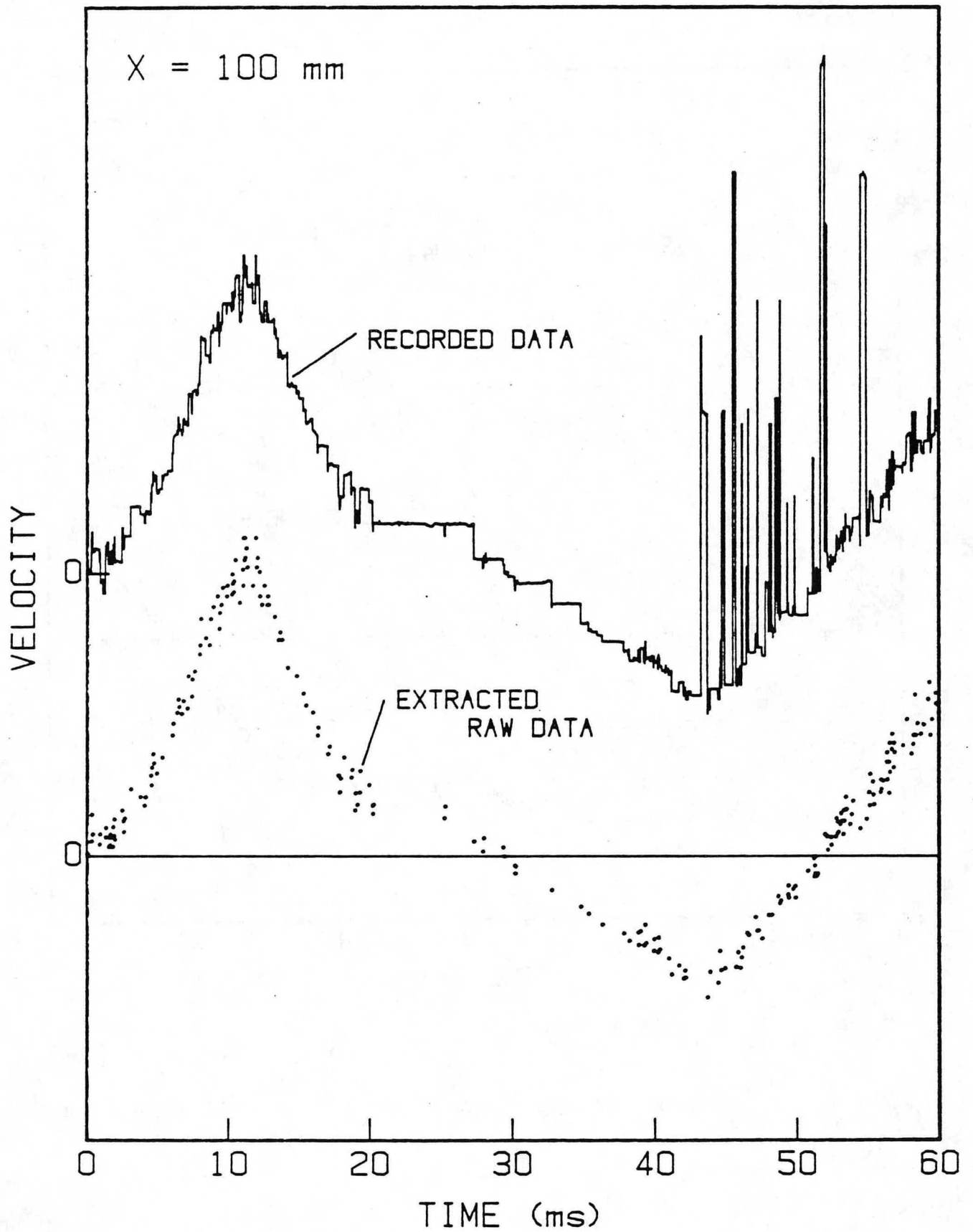


FIGURE 3. COMPARISON OF RECORDED DATA TO THE EXTRACTED RAW DATA POINTS.

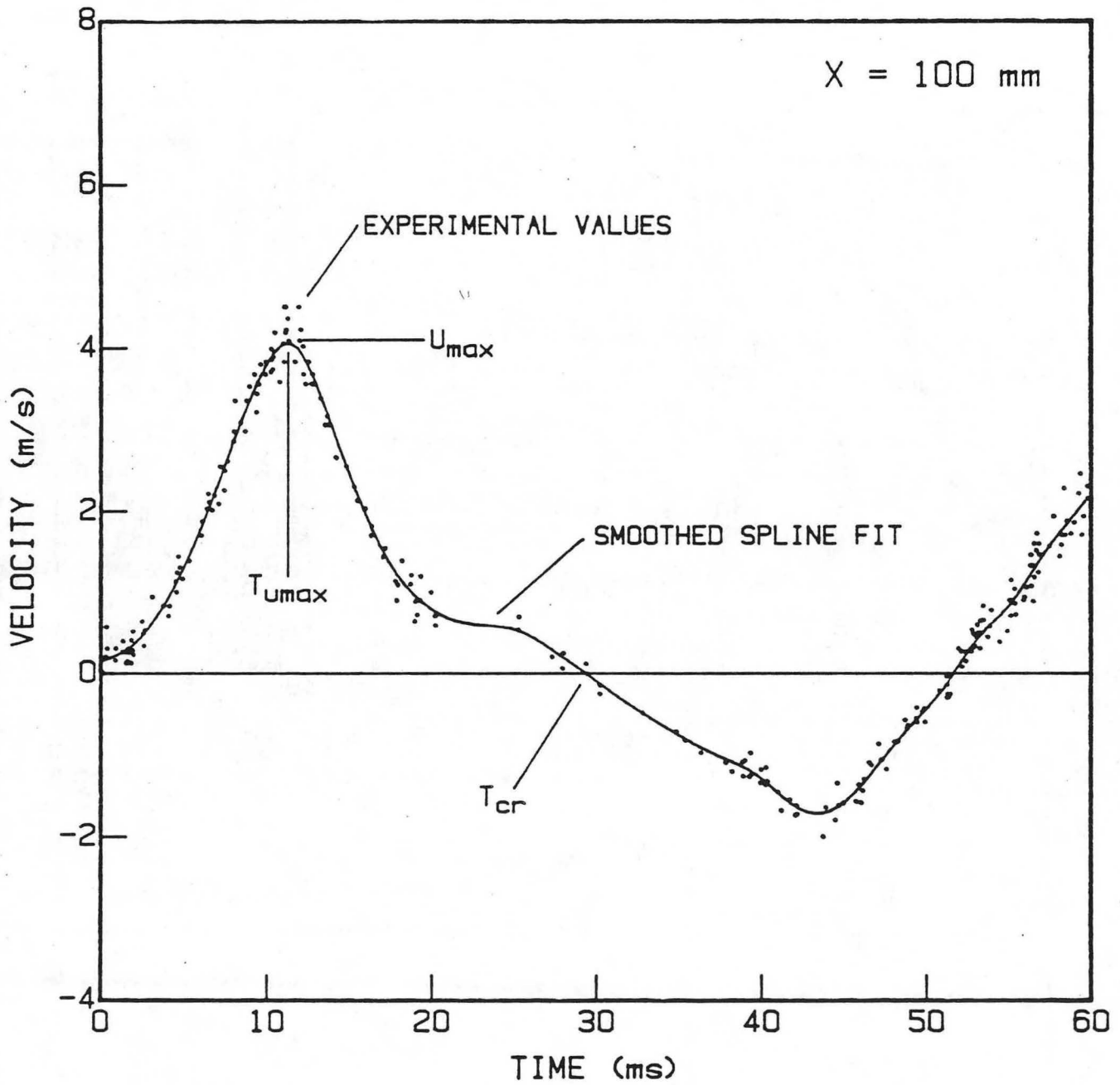


FIGURE 4. COMPARISON OF DATA POINTS TO SMOOTH SPLINE FIT. X = 100 mm.

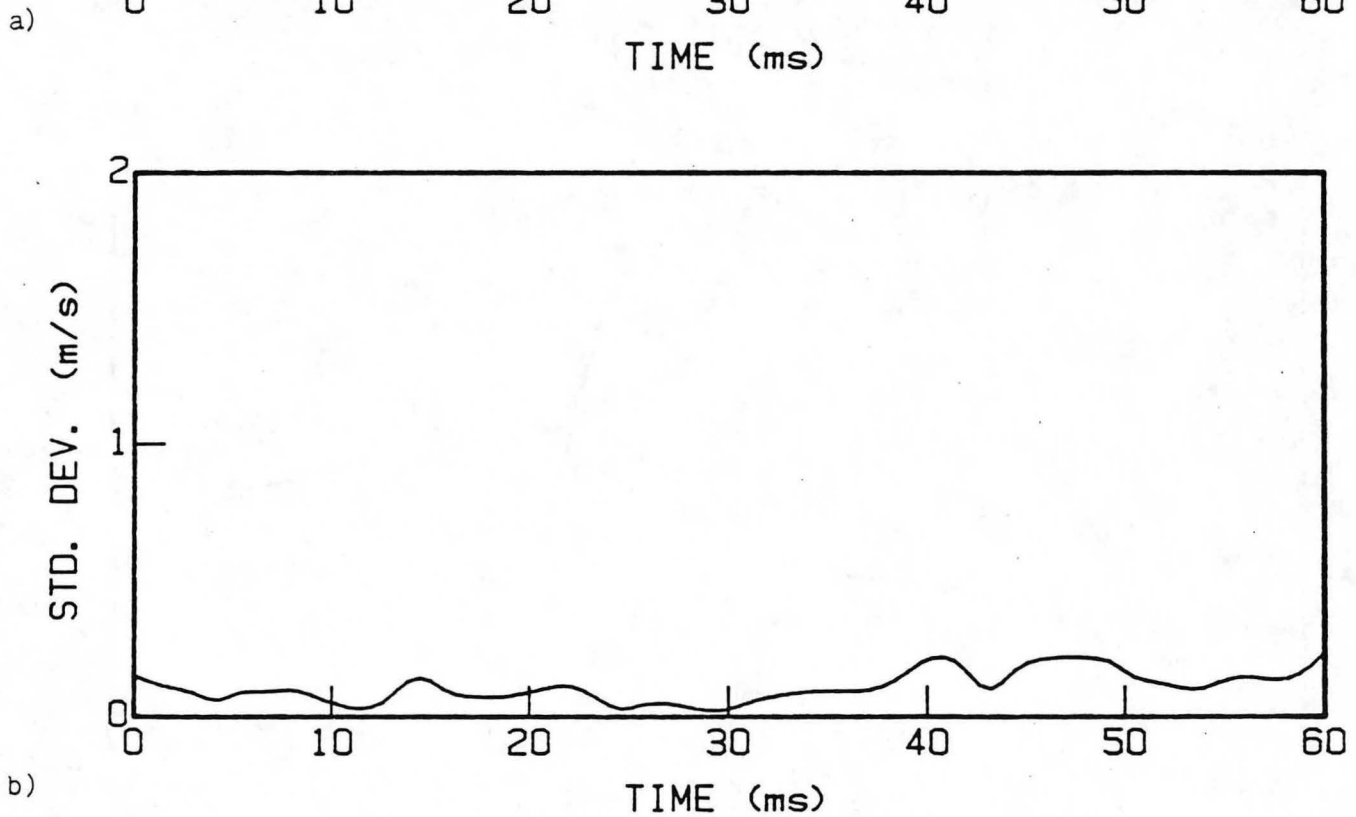
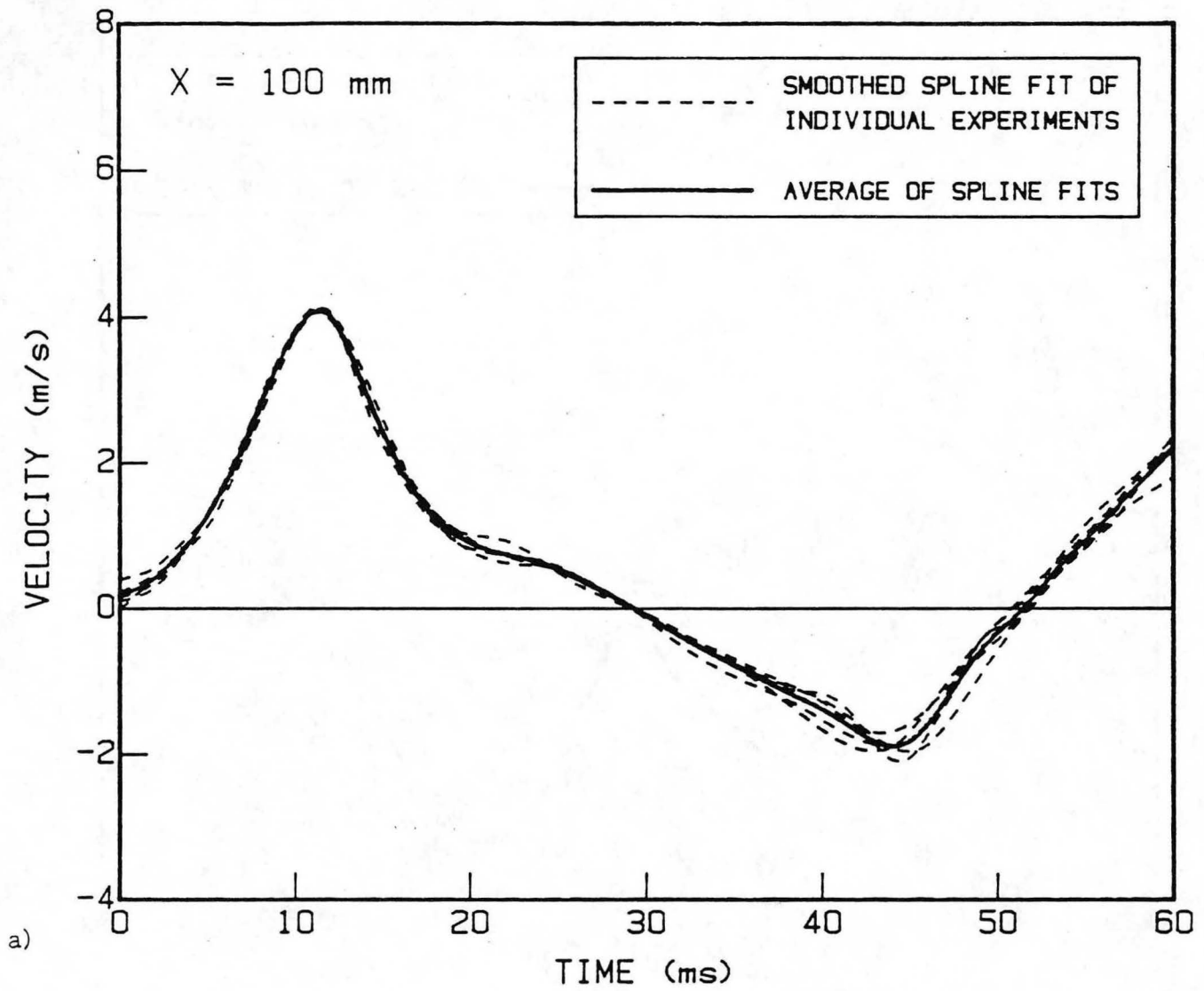


FIGURE 5. $X = 100$ mm. a) COMPARISON OF INDIVIDUAL SMOOTH SPLINE FITS TO THE AVERAGE OF FITS. b) STANDARD DEVIATION OF THE SMOOTH SPLINE FITS ABOUT THE AVERAGE FIT. TYPICAL FOR $X > 80$ mm.

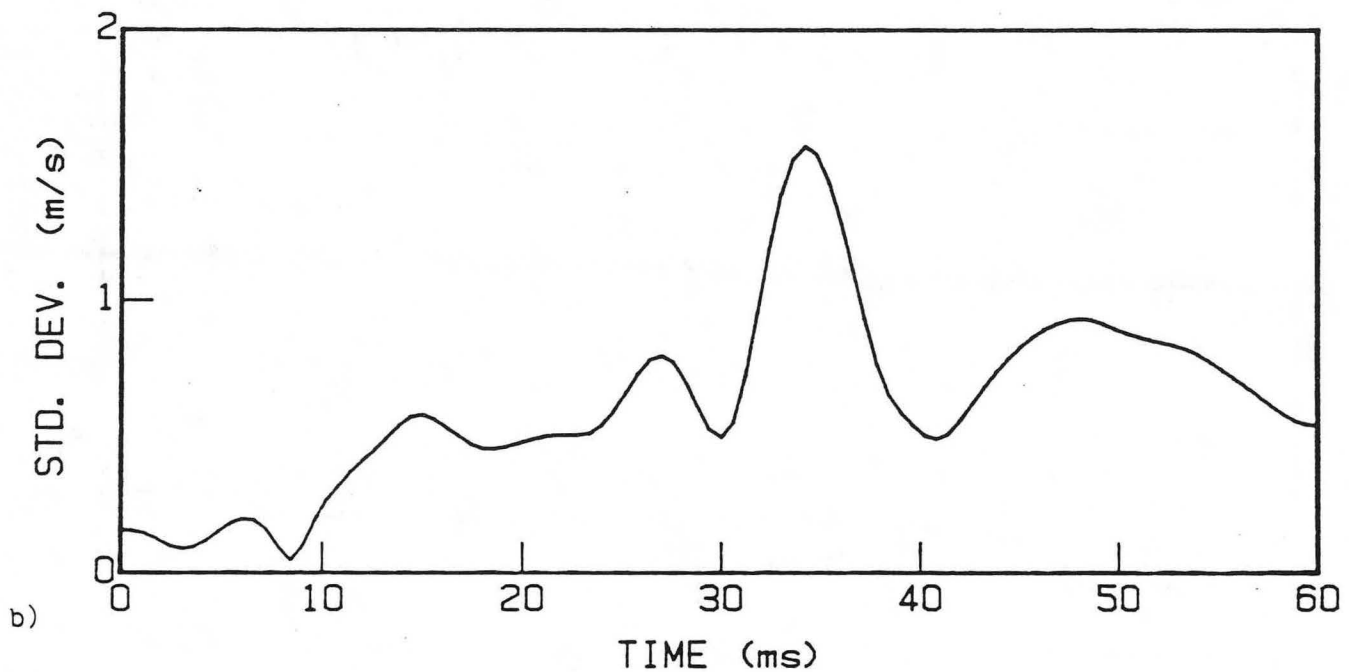
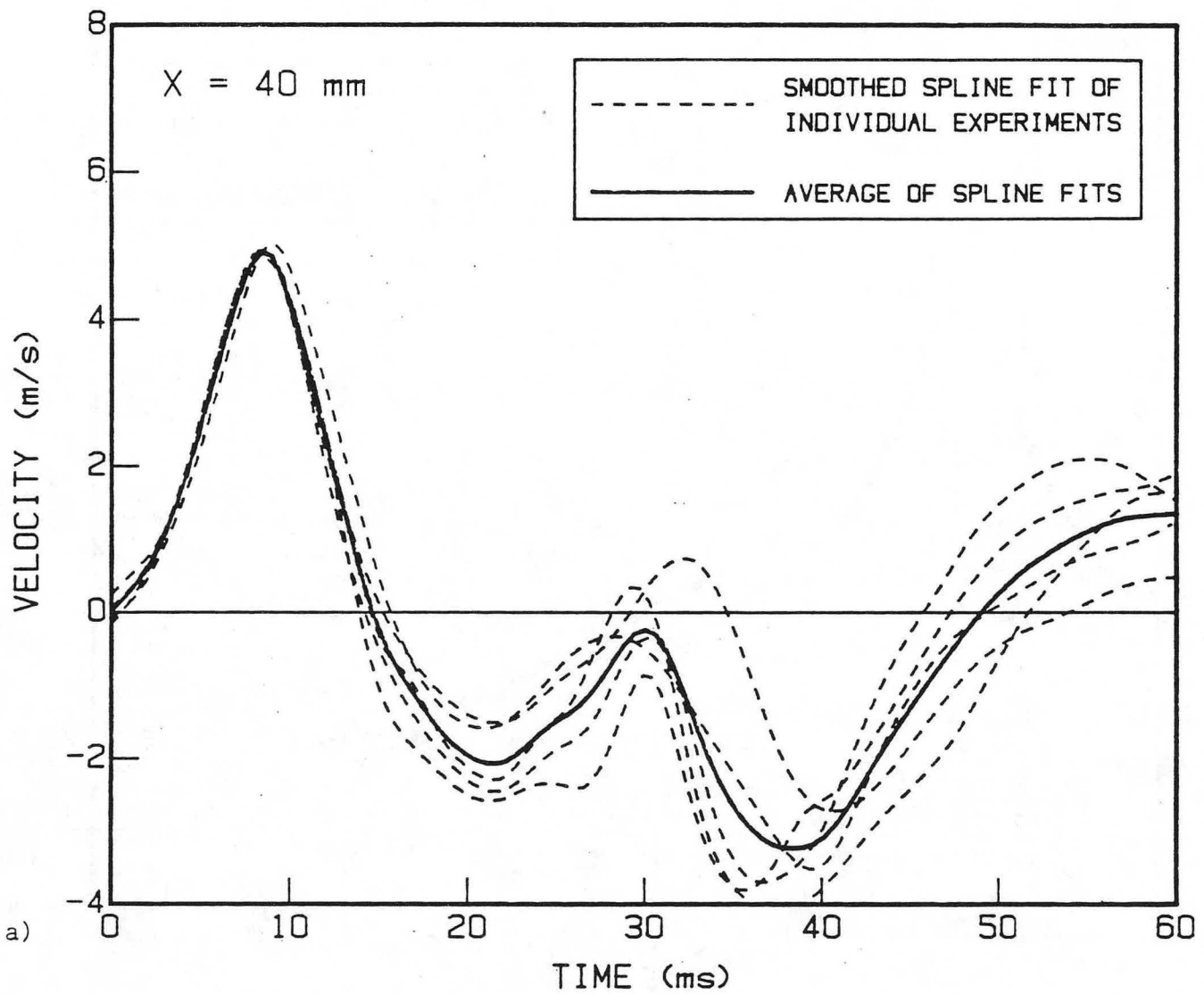


FIGURE 6. $X = 40 \text{ mm}$. a) COMPARISON OF INDIVIDUAL SMOOTH SPLINE FITS TO THE AVERAGE OF FITS. b) STANDARD DEVIATION OF THE SMOOTH SPLINE FITS ABOUT THE AVERAGE FIT. TYPICAL FOR $X < 80 \text{ mm}$.

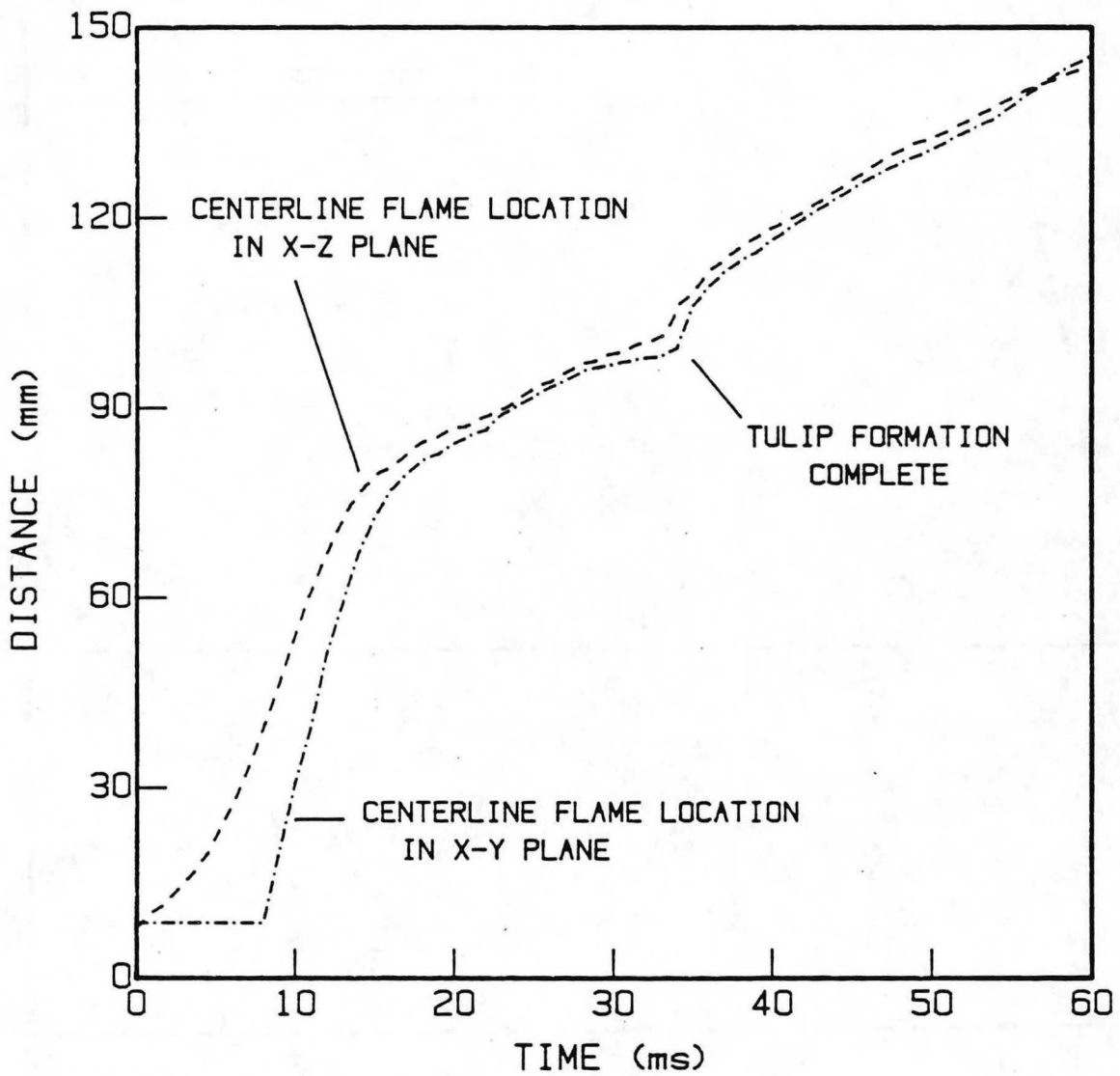


FIGURE 7. CENTERLINE FLAME TRAJECTORY FROM TWO ORTHOGONAL DIRECTIONS.

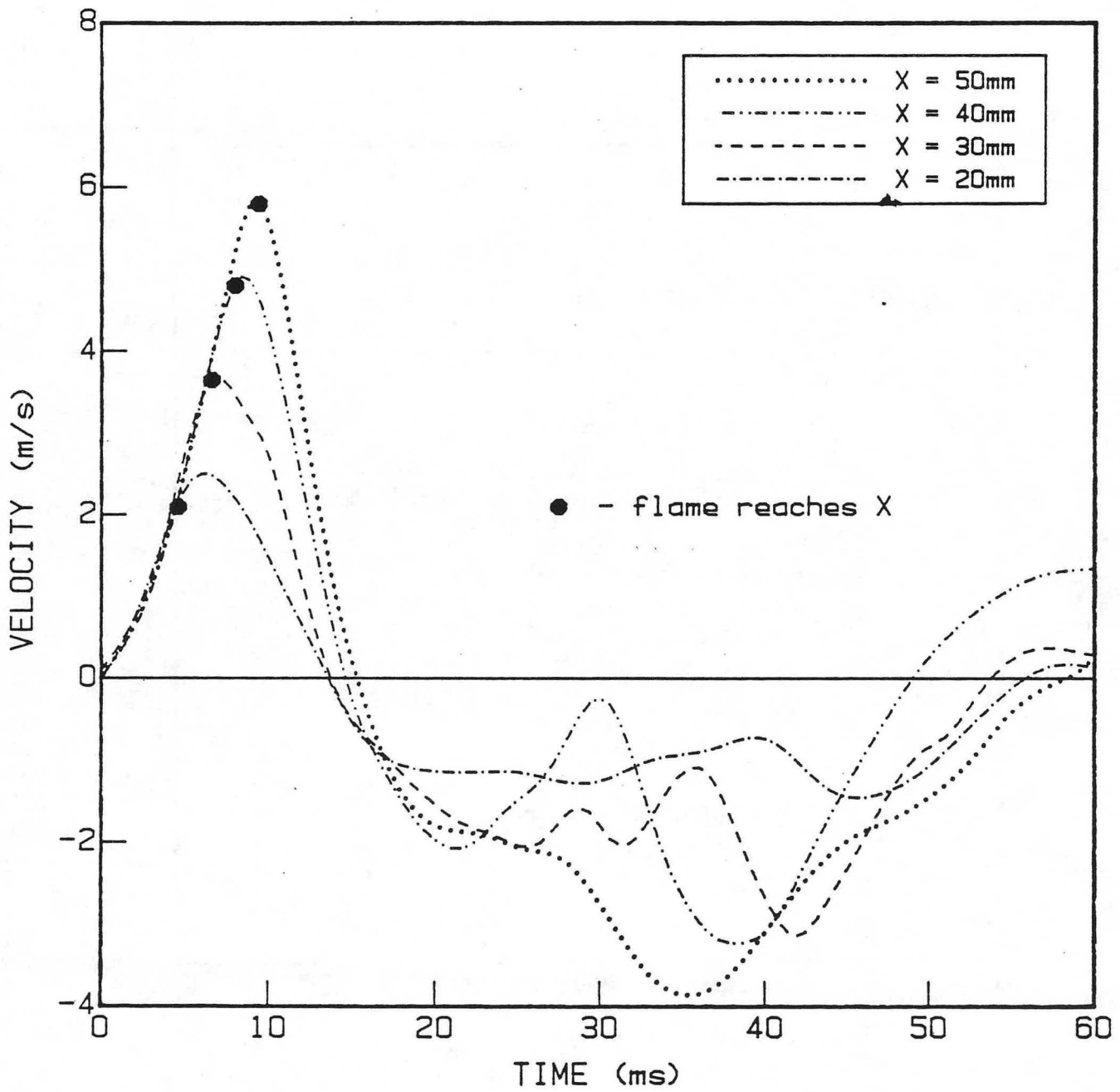


FIGURE 8a. CENTERLINE AXIAL VELOCITY/TIME RECORDS FOR $X < 50$ mm (group 1).

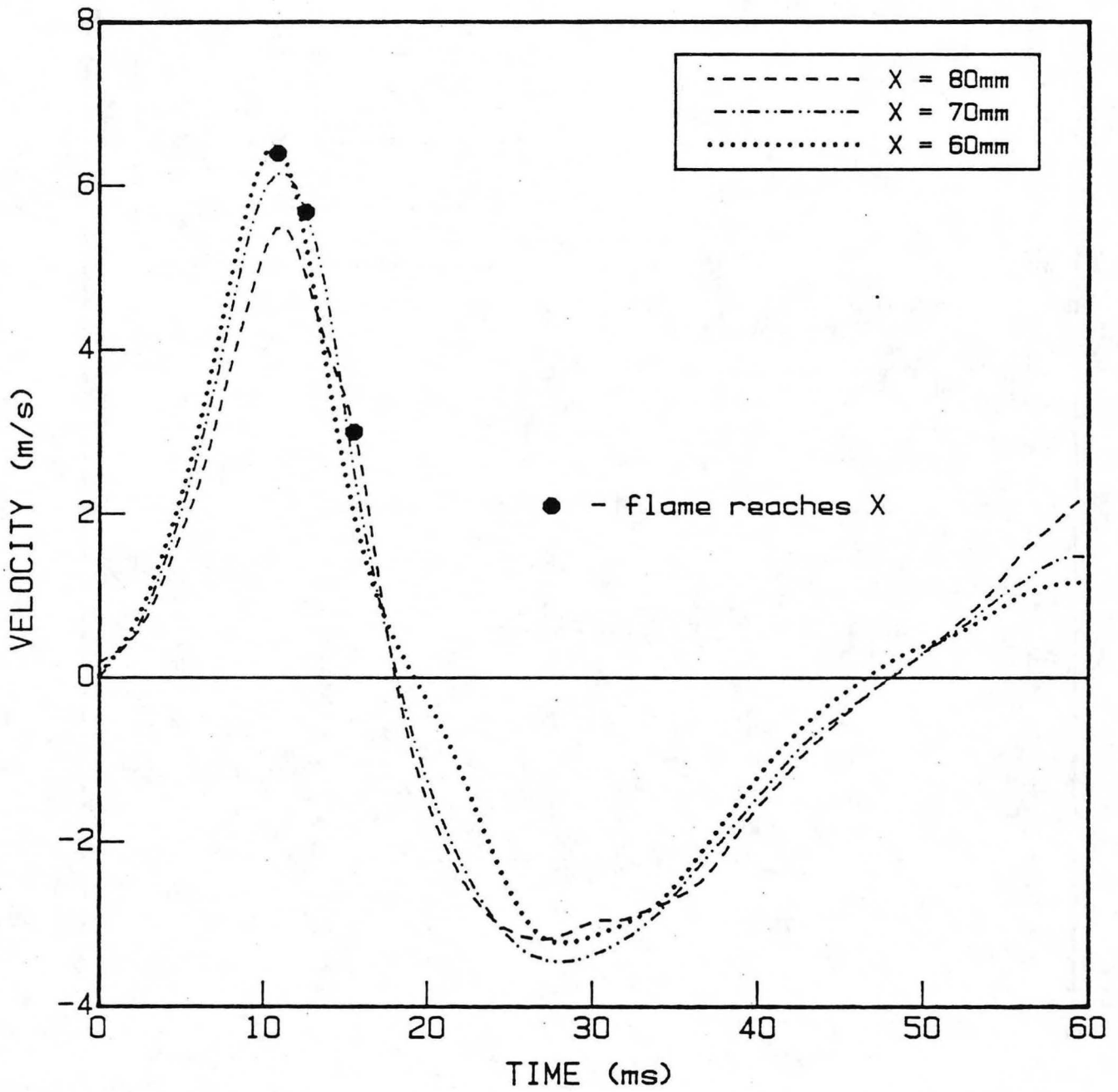


FIGURE 8b. CENTERLINE AXIAL VELOCITY/TIME RECORDS FOR 60 mm < X < 80 mm (group 2).

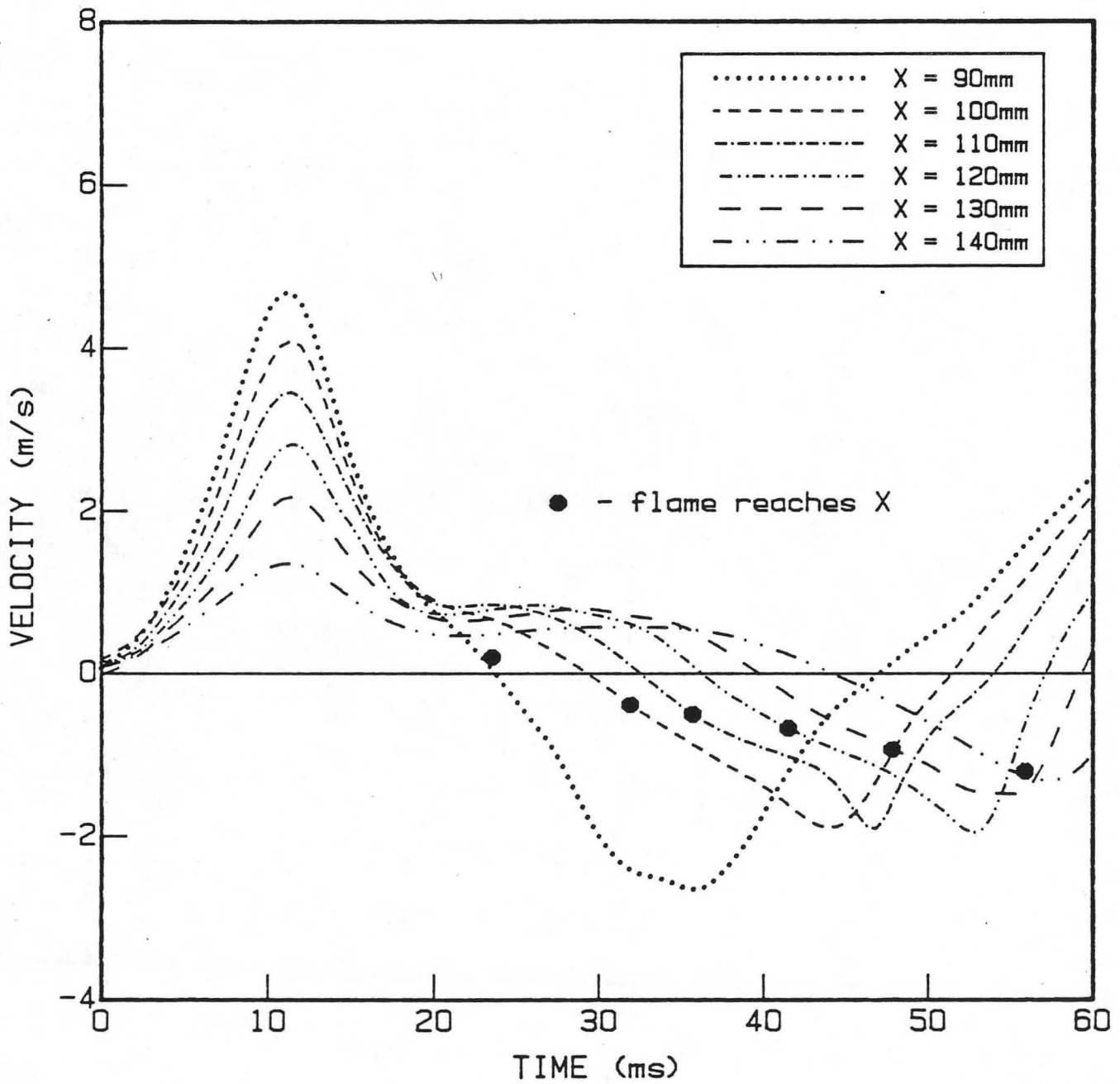


FIGURE 8c. CENTERLINE AXIAL VELOCITY/TIME RECORDS FOR $X > 90$ mm (group 3).

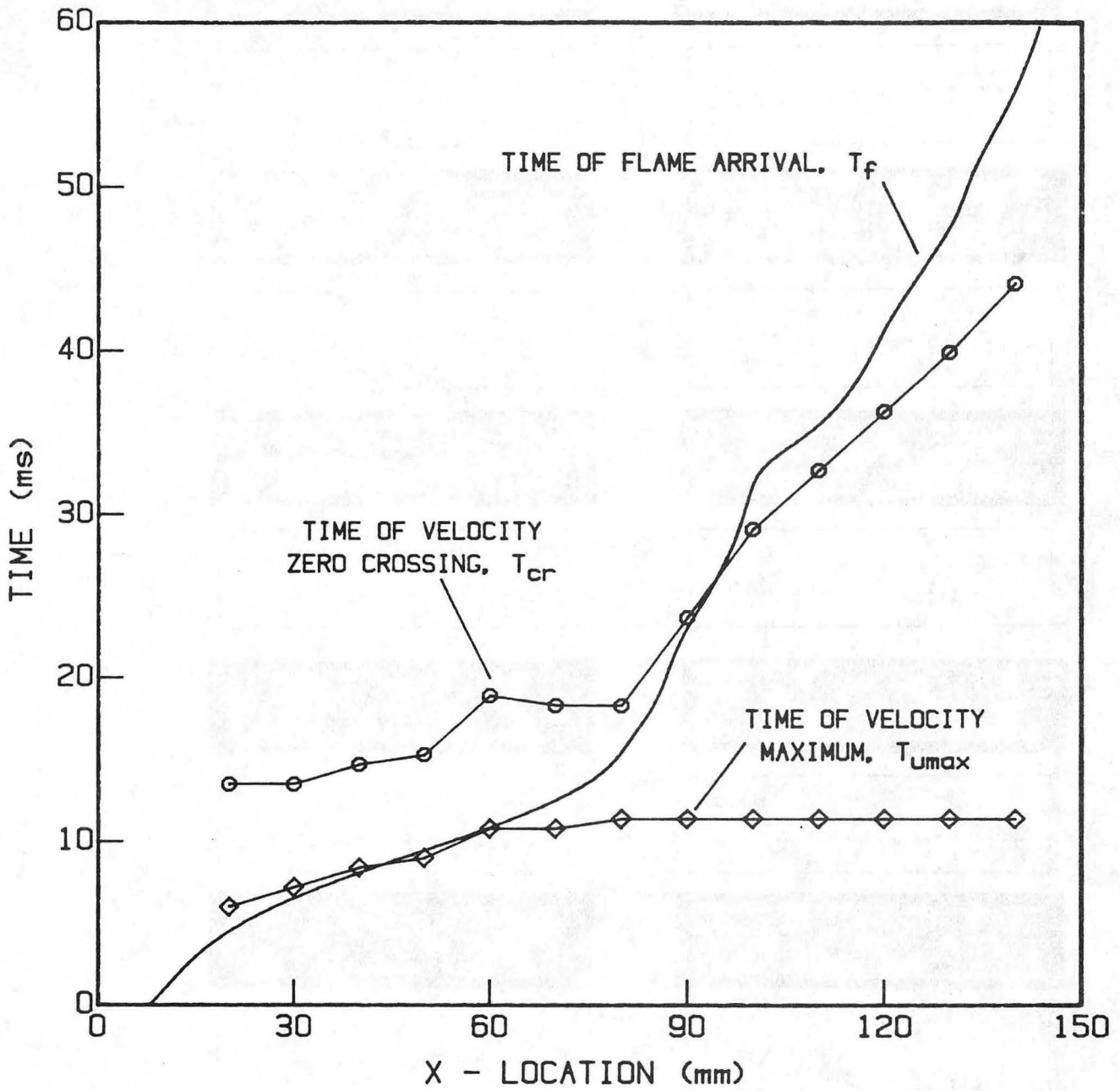


FIGURE 9. COMPARISON OF TIME OF FLAME ARRIVAL TO TIME OF VELOCITY ZERO CROSSING AND TIME OF VELOCITY MAXIMUM AT EACH MEASUREMENT POINT.

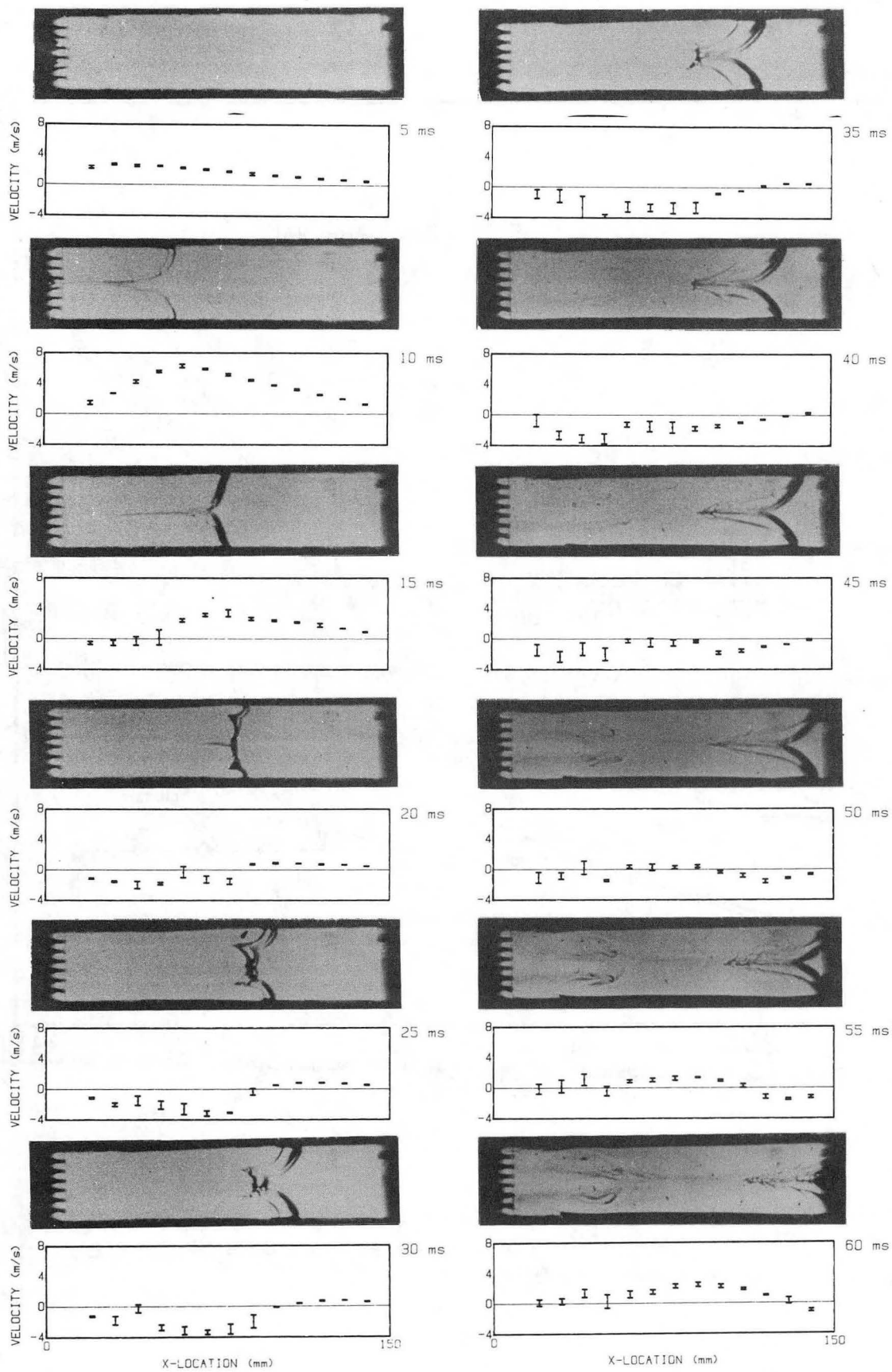


FIGURE 10. COMPARISON OF FLAME SHAPE AND CENTERLINE VELOCITY PROFILES AT VARIOUS TIMES.

This report was done with support from the Department of Energy. Any conclusions or opinions expressed in this report represent solely those of the author(s) and not necessarily those of The Regents of the University of California, the Lawrence Berkeley Laboratory or the Department of Energy.

Reference to a company or product name does not imply approval or recommendation of the product by the University of California or the U.S. Department of Energy to the exclusion of others that may be suitable.

TECHNICAL INFORMATION DEPARTMENT
LAWRENCE BERKELEY LABORATORY
UNIVERSITY OF CALIFORNIA
BERKELEY, CALIFORNIA 94720